Powder Technology 364 (2020) 484–493

Contents lists available at ScienceDirect

Powder Technology

journal homepage: www.elsevier.com/locate/powtec

Theoretical analysis of erosion in elbows due to flows with nano- and micro-size particles

Anna Kosinska [a,*], Boris V. Balakin [a,c], Pawel Kosinski [b]

[a] Western Norway University of Applied Sciences, Department of Mechanical and Marine Engineering, Norway
[b] Department of Physics and Technology, University of Bergen, Norway
[c] Department of Thermal Physics, National Research Nuclear University, Moscow Engineering Physics Institute, Russian Federation

ARTICLE INFO

Article history:
Received 20 August 2019
Received in revised form 25 January 2020
Accepted 1 February 2020
Available online 5 February 2020

Keywords:
Erosion
Nanofluids
Modelling
Theoretical analysis
Collisions
Multiphase flows
Contact mechanics

ABSTRACT

The present paper focuses on the issue of erosion due to fluid flow laden with nano- and microparticles. We investigated the case of a pipe elbow using theoretical analysis and numerical simulations. For the case when the particles were large, that is, of micrometre size, we observed the expected behaviour in which the erosion rate was greater with increasing particle diameter. The same was seen for flow velocity, and higher velocities promoted the erosion process. For small particles, however, the erosion rate increased with decreasing particle size. This was explained by the formation of secondary flows in the elbow that centrifuged the particles towards the walls. For very small particles, the erosion rate decreased again, i.e. the particle distribution towards the wall was insufficient to erode the pipe wall due to the particles low mass.

1. Introduction

Erosion of pipelines due to the transportation of very fine particles in fluids occurs in different branches of industry. A typical example is the petroleum industry where sand particles move through the system during oil and gas production. Very large particles are filtered by various techniques, e.g. sand screens, while much smaller particles move farther along in the system (see [1]). These particles can lead to pipeline wear and to subsequent damage.

The issue of particle erosion on pipes has been intensively researched in the scientific literature. The focus has usually been on elbows because they are frequent in systems and because the erosion is much more prominent than in straight sections of pipe due to the sudden change of flow direction. In addition, several different physical phenomena occur in such geometries, and this makes the process quite complex and interesting.

Liu et al. [2] investigated the flow of sand particles in a slurry using both experimental and numerical techniques. Their first observation was that the erosion rate was greater for higher velocities, but they also reported that changing the velocity resulted in moving the eroded region to other points in the pipe. This interesting observation could be explained by the formation of secondary flows in the system, and this observation is also relevant for our research.

Various mathematical models of erosion have been developed including those of Neilson and Gilchrist [3], Grant and Tabakoff [4], Oka et al. [5], DNV-model [6], Zhang et al. [7] or Mansouri [8], and there have been attempts in the literature to compare these models. One example is the work by Parsi et al. [9] who considered a flow where the continuous phase consisted of both a liquid and a gas phase. The issue was also studied by Song et al. [10] who focused on the particle trajectories in the system. Zamani et al. [11] showed the importance of including particle rotation in mathematical models, an issue often neglected by many researchers. Banakermani et al. [12] considered elbows where the angle varied between 15° and 90°, which led to interesting observations regarding erosion distribution. The paper by Zhou [13] focused on the influence of particle shape, that is, they also considered non-spherical particles in their modelling, and a similar approach was taken by Zeng et al. [14] in their theoretical research.

In addition, there have been works where focus was on other applications, for instance, erosion due to jet impingement [15–19], in a heat exchanger [20], in cyclones [21,22], and in a rectangular aperture [23]. Finally, our previous work focused on high-speed velocities [24], even though the exact process of erosion was not elucidated.

An interesting issue, which is the main focus of this paper, is the flow of so-called nanofluids, i.e. fluids immersed with metallic

* Corresponding author.
E-mail address: anna.dorota.kosinska@hvl.no (A. Kosinska).

https://doi.org/10.1016/j.powtec.2020.02.002
0032-5910/

nanometre-size particles [25]. Such fluids exhibit enhanced thermal properties and this makes them excellent candidates for many practical applications (e.g. fuel cells, microelectronics, and combustion engines). Recently, nanofluids have gained much interest in the field of solar energy [26,27].

Because nanofluids can potentially replace pure liquids in many applications, it is important to understand how nanofluids influence erosion processes. This is a crucial problem to address in order to avoid damage to the equipment due to the flow of the particles.

As mentioned previously, many researchers have analysed the influence of particle size on the erosion processes, and the general expectation is that smaller particles lead to less erosion. Nevertheless, using systems with particles of small diameter increases their number in the system for a specified volume concentration, which might enhance erosion. In addition, these small particles can more easily penetrate into regions that the larger particles cannot enter.

In most practical applications, flows contain particles of at least micro-size. Nevertheless, nanofluids have gained significant interest in recent years so that it should be investigated how flows laden with nanoparticles erode the walls of pipelines.

The erosion wear due to nanofluids has been not widely studied in the literature. However, one example is the work of Shamshirband et al. [28], who investigated the process of particles of both micro- and nano-size in fluids flowing through elbows. The main objective of their paper was the development of a numerical scheme (an adaptive neuro-fuzzy inference system), which makes their paper slightly less relevant to our research. Also, as described below, they focused on a different range of flow velocities than we did.

Another example is the work of Safaei et al. [29], who studied flows laden with both micro- and nanoparticles through elbows. Their results confirmed the expectations that particles of greater diameter and moving with greater velocities in such systems will result in greater erosion rates.

In addition, there have been works where the focus was on flows of nanofluids and investigating the resulting erosion, but not necessarily in elbows. Some examples are the paper by Asifa [30], who analysed flows in radiator pipes, and the paper by Molina et al. [31], where the focus was on surfaces subjected to jets of nanofluids.

The present is solely theoretical and takes two approaches to the issue of erosion due to nanofluids. The first is an analysis of the erosion process where nano-size particles are present in the system. As in many previous papers, the focus is on flow through an elbow, and our objective is to predict the outcome by considering the main process parameters.

The second approach focuses on numerical experiments where the particles present in the fluid flow erode the pipe walls. We consider a wide range of particle sizes starting from particles of micrometre-size to particles of nano-metre size (i.e. nanofluids in the latter case). Our main finding is that there is a sudden increase in pipe erosion as the particle size decreases, but then there is a decrease in erosion when they reach nanoparticle size.

2. Approximate analysis

The first issue addressed by many researchers was the effect of particle diameter on the erosion rate [16,19,32]. Generally, it is known that small particles erode pipelines less than large particles because they have a lower mass. As a result, their kinetic energy is also less such that pipe wall erosion might be expected to be negligible for very small particles. However, smaller particles are also associated with higher number concentrations of particles. In other words, for a given volume fraction of particles in a fluid, the number of collisions with the surfaces will increase as the particle diameter decreases. Assuming the particles to be spherical, we can relate numbers of particles in a unit volume:

$$N_1 = N_2 \cdot (D_2/D_1)^3, \tag{1}$$

where N_1 and D_1 are, respectively, the number of particles and their diameter when the particles are "small" (e.g. nanoparticles). Similarly, N_2 and D_2 describe "large" particles (e.g. particles of micrometre-size). This means that when moving from micrometre-size particles to nanometre-size particles (2–3 orders of magnitude difference), the number of particles increases by 6–9 orders of magnitude.

Further, we assume that the erosion rate of a single collision between a particle and the wall depends on the particle size according to D^m, where m is a coefficient being 0.3–2.0 [1,32]. Thus, for N particles in the system the erosion rate ER becomes:

$$ER \propto N \cdot D^m. \tag{2}$$

Alternatively, when comparing the erosion rates between nanoparticles and microparticles:

$$ER_1/ER_2 = N_1/N_2(D_1/D_2)^m. \tag{3}$$

Assuming N_1/N_2 to be on the order of 10^6 and D_1/D_2 to be on the order of 10^{-2} (see the discussion under Eq. (1)) and m being equal to 1.0, the erosion rate should increase 10^4 times according to Eq. (3). This indicates that erosion can be quite significant for very small particles, i.e. nanoparticles.

It must be noted, however, that smaller particles usually track the fluid flow due to their low inertia when compared with larger particles. This means then when flowing through, for instance, elbows, the larger particles will be more likely to collide with the walls than nanoparticles. Therefore, the true particle-wall collision rate should be lower for nanofluids. In other words, an increase in the erosion rate by a factor of 10^4 cannot be realistically expected in many types of flows and geometries.

We can state that the collision rate depends on the Stokes number, which is defined as the ratio of the particle momentum response time (τ_v) and some characteristic time of flow (τ_F). The momentum response time (see, for example, [33]) is defined as $\tau_v = \rho_d D^2/(18\mu)$, where ρ_d is the particle material density and μ is the fluid viscosity. The characteristic time of flow can be estimated as the average flow velocity divided by the pipe radius. Alternatively, as shown later in the paper, it can also be estimated as the ratio of the flow velocity in a vortex or coherent structure and the radius of the vortex if the particles flow through the vortex.

This shows that the Stokes number is $\propto D^2$ and we can state that for high values of the Stokes number, the particles do not follow the flow easily and thus readily collide with the elbow surface, i.e. the number of collisions is high. Similarly, for very low values of the Stokes number, the number of collisions is reduced because the particles follow the flow of the fluid. Therefore, it can also be assumed that the collision rate is $\propto D^2$.

If we compare small and larger particles, where D_1/D_2 is of the order 10^{-2}, i.e. as in the analysis above, we find that the collision rate is less than 10^4 for the smallest particles. It is important to note that a similar factor was obtained above, but it worked in the opposite direction. Thus, there are two contradictory phenomena that respectively increase and decrease the erosion rate and the final total erosion rate depends on the studied problem and on the model used.

The process of erosion depends significantly on the flow velocity prior to the collision. The dependence is $\propto U^n$ for a single-particle wall collision. For small particles, U corresponds to the fluid velocity because these particles follow the fluid flow, as mentioned previously. When the flow changes direction and the particles are larger, however, there is a difference between the particle velocity and fluid velocity that might be impossible to determine by using purely theoretical analysis.

When increasing flow velocity in a piece of geometry where the flow direction changes (e.g. elbows), the Stokes number will also increase

because the characteristic time of the flow decreases. Therefore it is more difficult for particles to follow the flow and as a result, more collisions with the walls will occur. In the end, the erosion rate will also be higher.

Our results suggest that there are two phenomena that promote the erosion at higher velocities - (i) the inherent increase in the erosion rate when single particles collide with high velocity, and (ii) the increase in the collision rate.

An interesting issue is the influence of the collision mechanism on the erosion process, namely the coefficient of restitution. For particle-wall collisions, the coefficient of restitution is defined as the ratio of the post-collision and pre-collision velocities. This means that for an ideal elastic collision, this coefficient is 1.0, but in practice, the value less due to the loss of kinetic energy. This loss is caused by viscoelastic effects within the particle material, plastic deformation, etc.

If we now compare the two cases of high value of the coefficient of restitution and a low value, we can deduce that in the second case a particle will lose more of its kinetic energy when it collides with a wall. As a result, its next collision with, for example, the opposite wall will be with a lower velocity. Therefore, we could expect that the total erosion wear will be lower.

This is not necessarily the case when the particle diameter is small. After such a particle bounces off the wall, it will be quickly taken up by the main fluid flow and accelerated again. As a result, it will regain its kinetic energy and the next collision will not be any weaker than the previous collision. This will be the case for smaller particles, or generally the case for when the Stokes number is low. An important aspect is also the distance to the opposite wall or to another surface that the particle will travel to after the first impact.

In addition, an important issue when dealing with nanofluids is the possibility that the Knudsen number, defined as the ratio of the mean free path of the liquid molecules and the particle diameter, might exceed 0.001 [33]. This might influence the continuum assumption of the liquid, i.e. the so-called slip flow occurs. This indicates that for water molecules, for which the mean free path is equal to 2–3 Angstroms, the slip flow might begin to occur at particle diameters of 200–300 nm. In practice, however, the effects can probably be assumed to play a role for rather smaller diameters, perhaps an order of magnitude smaller. Therefore, we decided to disregard this issue in our research where only the smallest particles entered this region.

Finally, an interesting and complex phenomenon is the formation of agglomerates, which occurs especially if the particles are smaller. In the case of nanoparticles, they can form structures that are perhaps one or two orders of magnitude larger depending on the specific properties of the particle and the fluid. The agglomerates might lead to significantly different results because the more intense collisions with the walls, which would lead to increased erosion, are cancelled out by the decreased collision rate due to the smaller number of particles. It should be noted that this resembles the analysis performed above, see Eqs. (1–3).

Similarly, adhesion to the walls that form particle deposits will reduce the number of particles in the system. Thus, the erosion rate will decrease farther from the regions where the deposits are formed. Whether this problem occurs or not depends on the studied problem and the potential ability for the particles to adhere to the wall surface.

3. Mathematical model of the fluid flow

The second tool used in our research was the computational fluid dynamics technique as carried out with the commercial software StarCCM+. In the mathematical model used in this study, we assumed that the fluid flow (denoted as c) was described by the equations of continuity and momentum as (see e.g. [33]):

$$\frac{\partial \phi_c \rho_c}{\partial t} + \nabla \cdot (\phi_c \rho_c \mathbf{u}) = 0 \tag{4}$$

$$\frac{\partial \phi_c \rho_c \mathbf{u}}{\partial t} + \nabla \cdot (\phi_c \rho_c \mathbf{u}\mathbf{u}) = -\phi_c \nabla p + \nabla \cdot \left(\phi_c (\tau + \tau^t)\right) - f_\Sigma, \tag{5}$$

where ρ_c is the density, $\mathbf{u}$ is the velocity, p is the pressure, and τ and τ^t are the molecular and shear stress tensors, respectively. ϕ_c is the volume fraction that in the current paper was almost 1.0 due to the low particle concentrations. Nevertheless, it was included in the model.

In the model above, the interphase forces (e.g. the drag force) are described by f_Σ. There has been discussion in the literature, see e.g. [34–36], as to whether the erosion rate for flows in elbows is influenced by these forces. The effects of two-way coupling and one-way coupling have been compared, and the difference has been found to be minimal. Still, we considered the full two-way coupling in our research.

The fluid flow was turbulent, and it was modelled by the standard k-ϵ model. The liquid was water. For the boundary conditions, we selected the non-slip assumptions when modelling the flow close to solid walls.

The particles were modelled using the Lagrangian approach, which means that the particle motion was tracked in the computational domain. The mathematical model was Newton's second law:

$$m_{di} \frac{d\mathbf{v}_i}{dt} = \Sigma \mathbf{F}, \tag{6}$$

where i refers to the i-th particle, m_d is the particle mass and $\mathbf{v}$ is the particle velocity. In the model above, $\Sigma\mathbf{F}$ describes the forces acting on the particles. Two forces were considered in the model: the drag force (modelled using the Schiller-Naumann model) and the Saffman lift force. The models can be found in the literature, see for example, [33].

When modelling flows with very small particles, the effects of Brownian motion cannot be excluded. Also, in our recent publication [27], we considered the effect. This paper, however, focuses on rather larger particles. As shown later, the most interesting results were obtained for particles of micro-size, where the Brownian force does not play a major role. On the other hand, nanoparticles may still form larger agglomerates when flowing, that is, Brownian motion may indirectly influence the course of the process. Still, the present paper does not focus on agglomerate formation. Therefore, we did not include Brownian motion in our research.

In addition, we assumed that the particle concentration was rather low. This allowed us to neglect particleparticle collisions, which saved computational time. Of course, the presence of frequent collisions might also affect the erosion process in the flow. After collisions with the wall, some particles might collide with other particles and be pushed back towards the flow and thus increase erosion. On the other hand, an opposing phenomenon can also occur in which particles travelling towards a wall might be slowed or stopped by other particles already in close proximity to the wall. In other words, a shielding effect might take place such that the total erosion rate might be lower.

Particlewall interactions were considered by using a standard rebound model with two coefficients of restitution one along the normal and one along the tangential to the plane of collisions. For simplicity, both were assumed to be equal to 0.99 in most of our simulations. Also, the influence of these coefficients on the erosion process is described later in the paper.

The particle erosion with the wall of the pipe was modelled using the model by Oka et al., see [5,37]. The model can be described by the following relation:

$$E_f = \frac{1}{A_f} \sum \dot{m}_d ER, \tag{7}$$

where A_f is the area of the wall surface subjected to collisions, $\dot{m}_d$ is the mass flow rate of particles colliding with the surface and ER is the erosion ratio. This means that the model computes the erosion rate: the mass of wall eroded per unit area and per unit time.

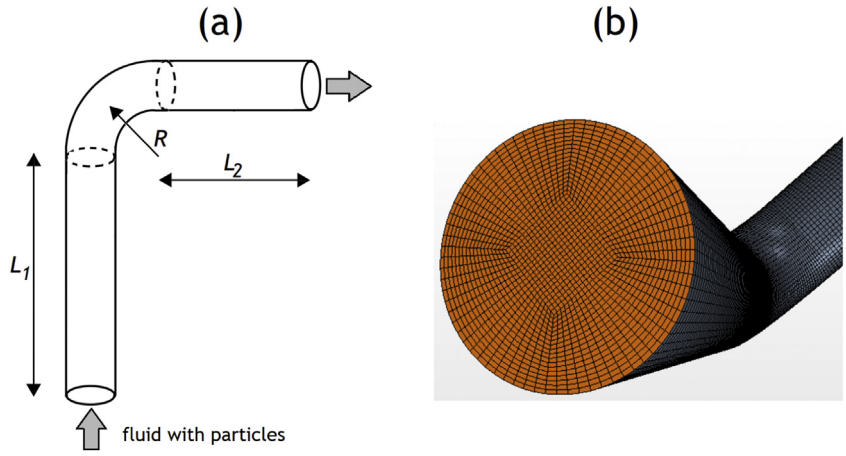

Fig. 1. (a) The geometry studied in this research; (b) The butterfly-type mesh used in the simulations.

The erosion ratio is calculated as [5]:

$$ER = (\sin\alpha)^{n_1}(1 + Hv(1-\sin\alpha))^{n_2} K \left(\frac{v_{rel}}{v_{ref}}\right)^{k_2} \left(\frac{D}{D_{ref}}\right)^{k_3}, \quad (8)$$

where n_1, n_2, K, k_2, and k_3 are constant parameters, Hv is the material hardness (units are GPa in the model), v_{rel} is the relative velocity of the particle with respect to the wall and is calculated along the normal to the collision plane, v_{ref} and D_{ref} are reference values (for velocity and diameter, respectively). In the end, α is the collision angle (measured from the normal to the impact plane).

In this research, we decided not to consider the influence of the empirical constants on the erosion processes, because this issue has already been widely studied in literature. Therefore we used parameters as inspired by the work of Oka et al., where $n_1 = 0.74$, $n_2 = 1.823$, $Hv = 1.34$ GPa, $K = 2.14{\cdot}10^{-4}$, $v_{ref} = 104$ m/s, $k_2 = 2.33$, $D_{ref} = 3.26{\cdot}10^{-4}$ m and $k_3 = 0.19$.

The erosion model was developed for particles of micro-size, while the present paper focuses also on particles of lower size. Nevertheless, it is challenging to find appropriate mathematical models in literature and therefore we adopted the existing model. On the other hand, we do not expect that this would significantly influence the conclusion of our research.

In this paper, we studied a geometry shown in Fig. 1a. In other words, the geometry resembles a typical piece of a pipeline with an elbow, studied by many other researchers. The pipe diameter d and curvature r were both 0.0508 m (i.e. 2 in.), and lengths l_1 and l_2 were 0.3048 m and 0.1524 m, respectively. The choice of the geometry and the input parameters was arbitrary but it should not influence the final observations and conclusions. The fluid laden with particles was injected from the inlet as seen in the figure.

The particle volume flow rate was in all cases as shown in Table 1. Hence, the flow was dilute so that an increase in the particle volume concentration should simply increase the total erosion rate due to the greater number of particles. Therefore, it was not necessary to study the effect of this parameter on the final results.

We assumed that the particles were made of silica. Because the fluid was water, this system mimicked a typical multiphase system used in many applications. We used different values of particle diameter, as shown in Table 1. Thus, the objective was to study both nanofluids and fluids with larger particles.

We considered four values for the inlet velocity, see Table 1. This range was sufficient to emphasise interesting observations, as described below. The corresponding Reynolds numbers were: 28524, 57,048, 85,572 and 114,096.

The simulation procedure was as follows: at first, the fluid with no particles was injected into the system with a specified velocity. The simulation was run until the flow became steady, that is, we could neglect any start-up effects. To assess this process, we monitored fluid velocity in a few selected points, as well as we observed visually the velocity profile in the main cross-section of the system. We chose 1.4 s as the point in time when the simulation terminated, but in practice, a steady flow was achieved much earlier. Afterwards, the particles were injected and the simulations were run until the flow became steady again. For this, we monitored the total erosion rate in the whole system: the steady case was stated to occur when we observed no change in the erosion rate for a longer period. We stopped the simulations after 4.7 s, and all of the results presented below correspond to this point in time.

The simulations were carried out using the SIMPLE technique with a time step 0.025 s (implicit, unsteady). The temporal discretization was first-order.

4. Results

4.1. Grid selection

For modelling of the flow, we selected the so-called butterfly mesh available in Star-CCM+. An example of this mesh is shown in Fig. 1b. It must be noted that a similar mesh was also used in [9,11,12], where the focus was on similar issues as in our work.

In our work, we tested the following number of mesh cells: 75000, 225,000 and 421,200 cells, and the final selection was made based on observation of the dimensionless value y + in the first layer of cells closest to the wall. The resulting distributions of y + on the pipe surface are shown in Fig. 2.

The y + value should be between 5 and 30 to ensure that the turbulence model is appropriate. According to these criteria, the last case led to satisfactory results even though we observed some high values of y + in some regions of the elbow. In addition, we tested the influence

Table 1
Input data used in the simulations.

Parameters	Value
Fluid velocity	0.5, 1.0. 1.5 or 3.0 m/s
Particle diameter	from 10^{-8} m (i.e. 10 nm) to 10^{-3} m
Coefficients of restitution	0.99 (most simulations), 0.80, 0.60
Particle volume flow rate	10^{-4} m^3/s
Particle material density	2650 kg/m^3
Fluid density	998 kg/m^3
Fluid viscosity	$8.887{\cdot}10^{-4}$ Pa·s

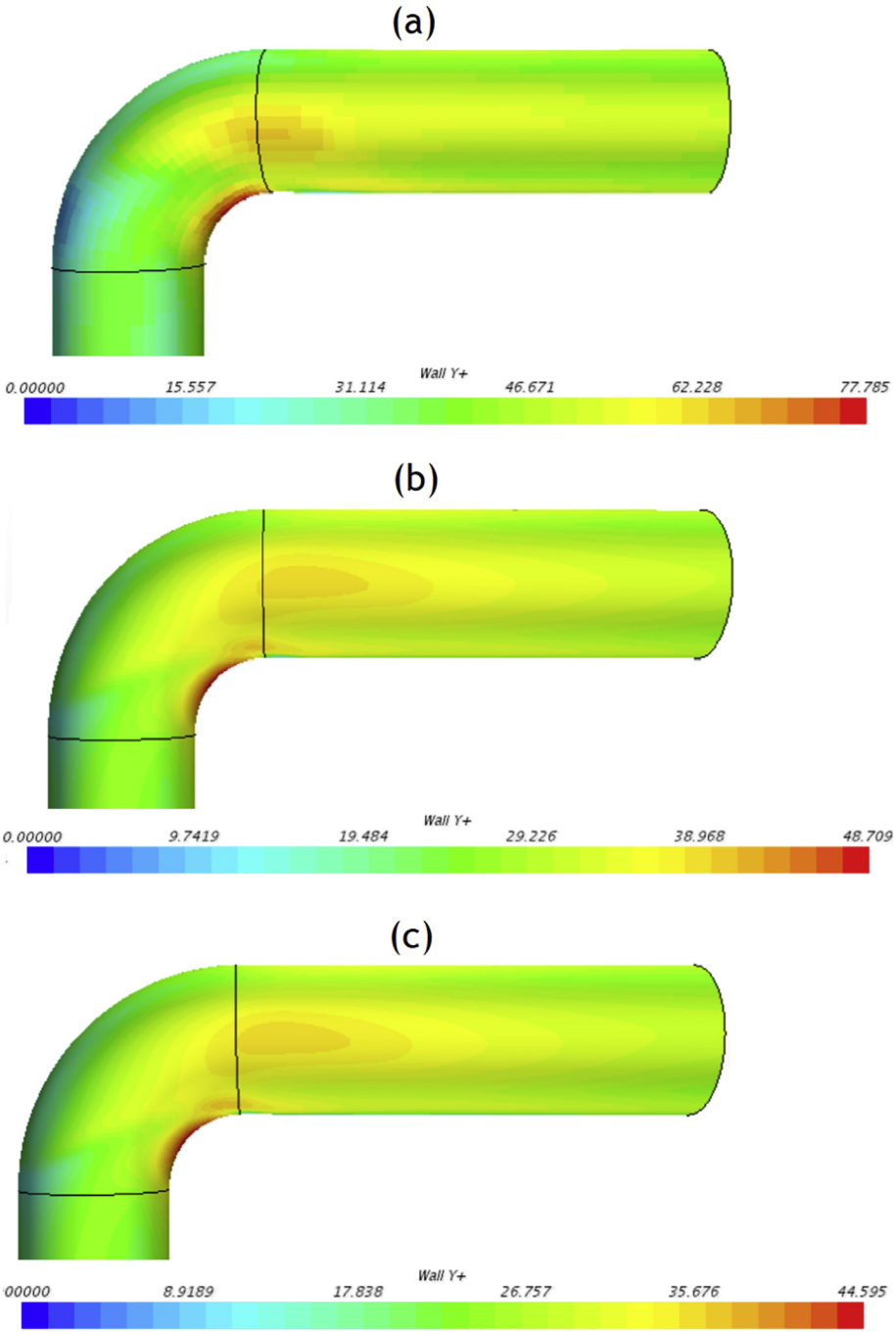

Fig. 2. Distribution of y + at the wall after the flow became steady using 225,000 mesh cells (a) and using 421,200 cells (b). Results are similar, but the finer mesh results in lower values of y+, which is preferable.

of the number of mesh cells on the total erosion rate in the elbow (for a particle size of 1.0 mm) and the results are compared in Table 2. According to the table, the results were similar and the case with 421,200 cells was selected for further analysis.

4.2. Software validation

The software and the models were further validated against experiments performed by Mazumder et al. [39]. They showed experimental results of a case where the pipe had inner diameter 25.4 mm, and the fluid was air and its velocity was 34.1 m/s at the inlet. There was injected 1.0 kg sand (modelled as silica in our paper) during 60 s, which corresponds to the volumetric flow rate 10^{-7} m^3/s. The particle diameter was 182 μm (see also [34]), and the coefficients of restitution were assumed to be 0.99. The erosion wear was measured on the extrados of the elbow in different locations described by an angle varying between 0 and 90 degrees.

Fig. 3 shows the comparison between our simulation results (the solid line) and the experiments (crosses), where the experimental results consist of three measurements. We show the dimensionless

Table 2
The total erosion rate vs. the number of mesh cells. All of the grids lead to similar results.

Number of cells	75,000	225,000	421,200
Total erosion rate [g/h]	$1.039 \cdot 10^{-3}$	$1.025 \cdot 10^{-3}$	$1.071 \cdot 10^{-3}$

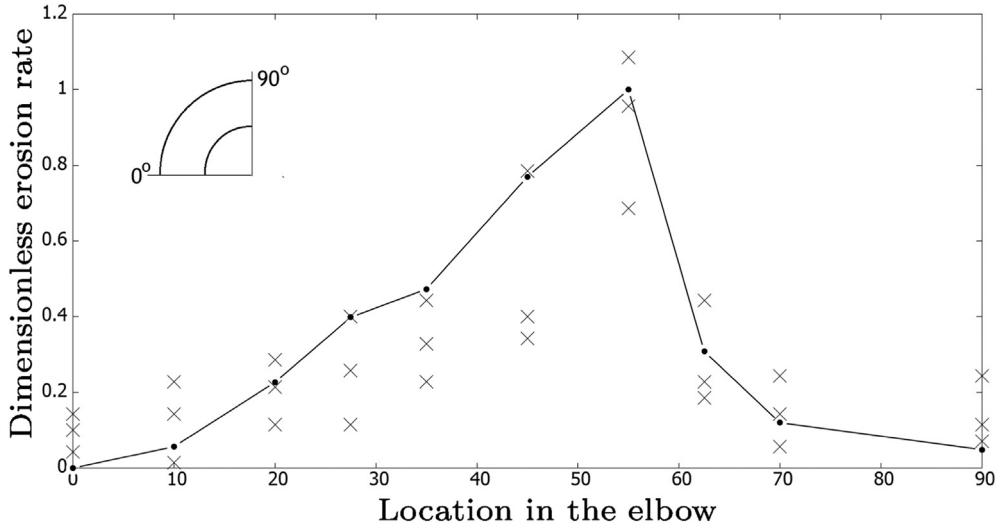

Fig. 3. Validation of the software: the dimensionless erosion rate for different locations in the elbow. The solid line corresponds to the simulation results, and the crosses are experiments by Mazumder et al. [39].

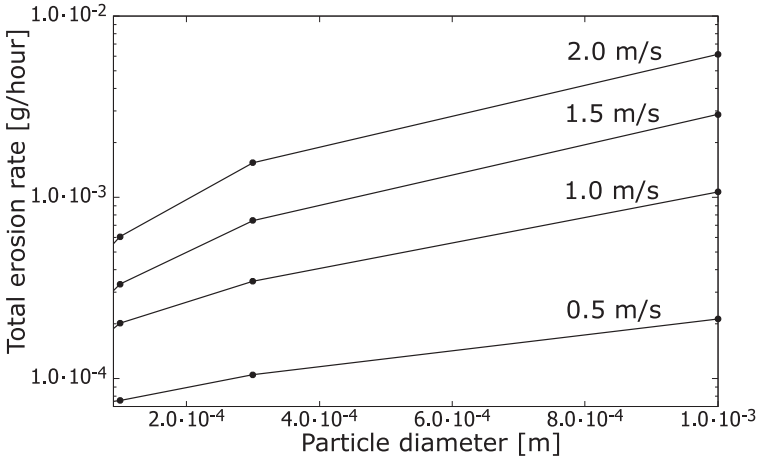

Fig. 4. The total erosion rate measured in the elbow after 1.4 s of the process (a steady flow was obtained) for three particle diameters. The focus is on the largest particles (the diameter was at least 150 μm.)

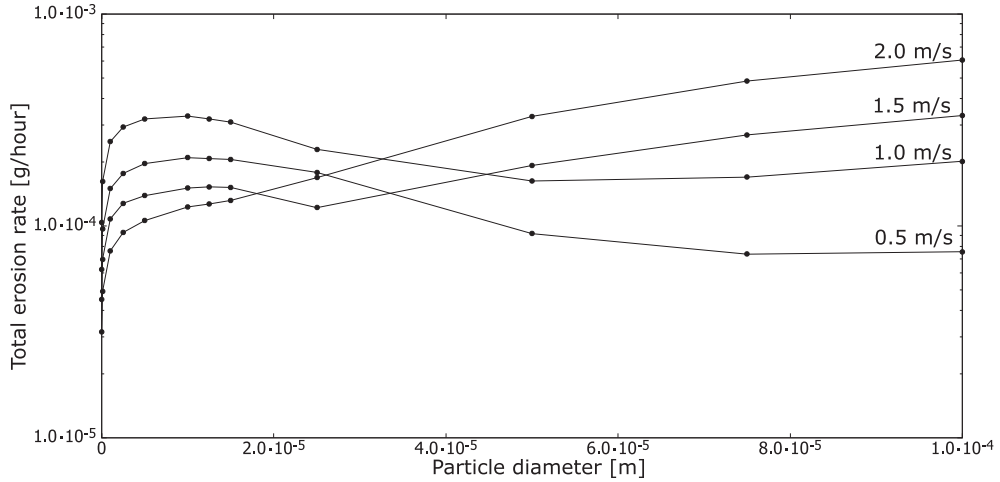

Fig. 5. The total erosion rate measured in the elbow after 1.4 s of the process (a steady flow was obtained) for various particle diameters. The focus is on the smallest particles with a diameter below 100 μm.

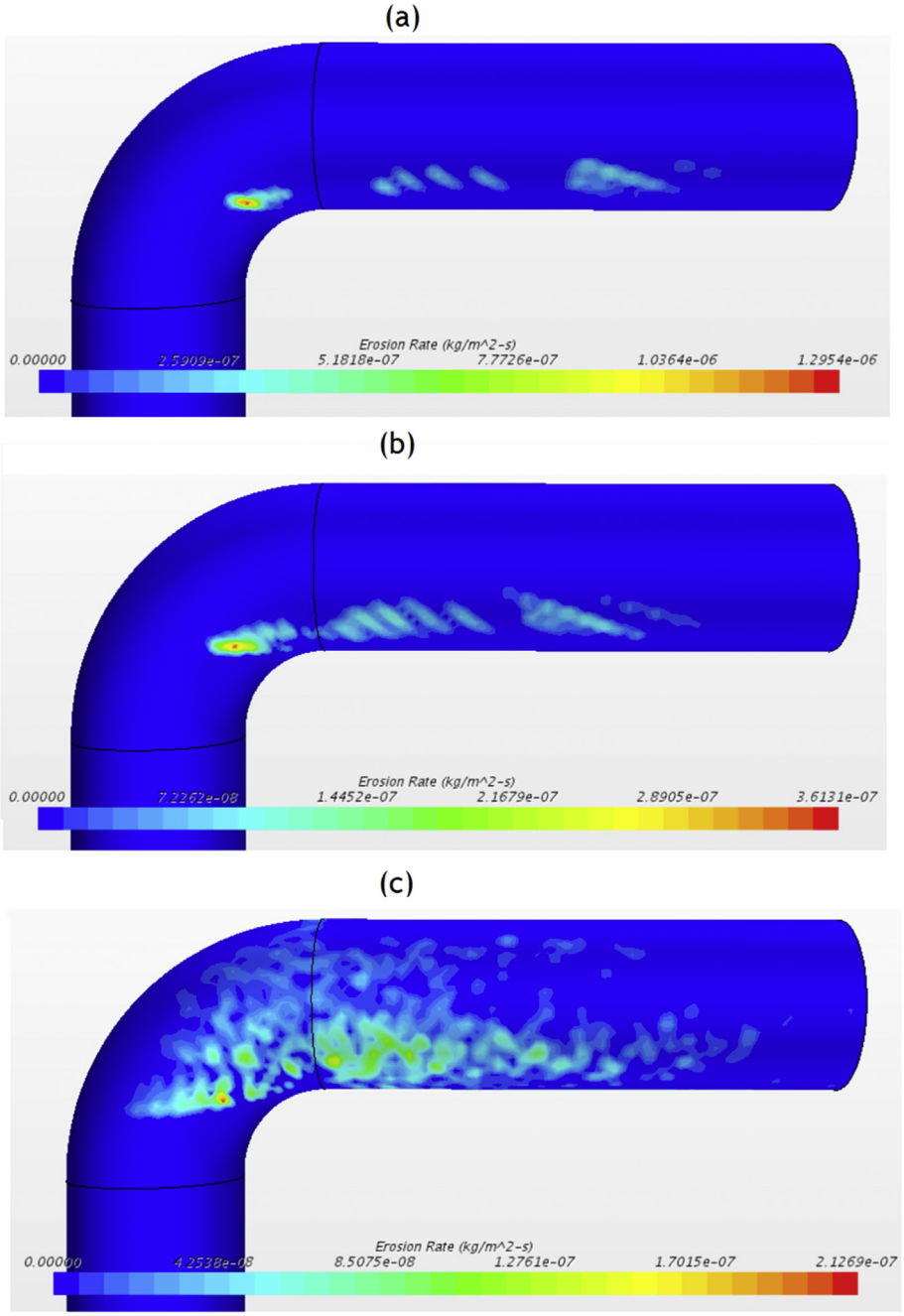

Fig. 6. Distribution of the erosion rate on the pipe surface for three particle diameters: (a) $1.0{\cdot}10^{-5}$m, (b) $5.0{\cdot}10^{-5}$m, and (c) $3.0{\cdot}10^{-4}$m. Fluid velocity was 1.0 m/s.

erosion rate that is the erosion rate obtained for a specific location with respect to the maximum erosion rate, which occurred for 55 degrees. It must be noted that Mazumder et al. showed the erosion wear in units of millimetres of removed pipe material that is directly proportional to the erosion rate used in this paper.

It is interesting to note that the correspondence is quite satisfactory, i.e. the mathematical model and the software could be used in the theoretical analysis shown in the following.

4.3. Influence of particle diameter and fluid velocity

The main objective of the present research was investigation to determine the influence of particle size on the erosion process. At first, we focused on particles of micro-size, that is, we repeated the work done by many other researchers. The results are shown in Fig. 4 where we compare not only the particle diameter, but also the initial injection velocity of the fluid laden with the particles. The total erosion rate increased with particle diameter and velocity, as expected. In other words, higher kinetic energy of the particles promoted erosion.

Next, Fig. 5 shows the influence of particle diameter and injection velocity for the case in which the particle size was smaller than what was previously studied, that is, the largest particles were around 100 μm. in diameter. In contrast to what we observed for the larger particles, we observed a decrease in the total erosion rate at some critical particle diameter (around $1.0{\cdot}10^{-5}$m). As the particle size decreased from this point, the total erosion rate increased until a second critical point was reached at which the erosion rate again decreased with decreasing particle size.

In order to describe this phenomenon, we analysed the data in Fig. 6 showing the distribution of the erosion rate on the surface of the pipe,

where three cases are depicted. We used different scales in the snapshots, because there are significant differences in the results. This was done to better elucidate the details of the process.

At, first we focus on the case where the particle diameter was $1.0{\cdot}10^{-5}$m (see Fig. 6a), i.e. this case corresponded to the local increase in the total erosion rate as seen in Fig. 5. It is clear from the figure that the pipe as a whole was not significantly subjected to erosive processes because the erosion primarily occurred in a concentrated region in the elbow.

Fig. 6b shows the case where the particle diameter was $5.0{\cdot}10^{-5}$m. This corresponded to the local minimum in the total erosion rate observed in Fig. 5. When comparing Fig. 6a and b, we see that the images of the erosion distributions are similar. Nevertheless, the maximum rates (see the legends) are larger for the first case. This indicates that the smaller particles were being pulled towards the pipe wall, which resulted in greater erosion.

Fig. 6c shows the erosion distribution when the particle diameter was $3.0{\cdot}10^{-4}$m. This was the case where the total erosion rate (from Fig. 5) was almost the same as when the particle size was $1.0{\cdot}10^{-5}$m. It is interesting to note that the erosion distributions on the pipe surface differed significantly. For both cases, we observed a spot where erosion was high, but for the case where the diameter was $3.0{\cdot}10^{-4}$m, the erosion was widely distributed on the pipe surface.

When comparing the influence of the flow velocity in the pipe, we found that the formation of the local maximum occurred for lower velocities (less than 2.0 m/s). This can also explain why this issue has not been widely studied by many researchers; they usually perform their experiments at higher velocities. The ratio between the maximum and the minimum of the erosion rate was around 2.8 for a velocity of 0.5 m/s, 2.0 for a velocity of 1.0 m/s, and 1.2 for a velocity of 1.5 m/s, which indicates that the phenomenon of the erosion rate increase for some critical diameter was greatest for the lowest velocities.

In addition, we detected a shift in the local minimum, and for lower velocities the minimum was seen for larger diameters. There was almost a linear relationship here if we compared particle diameter and the local minimum of the velocity, and this showed that the minimum does not really depend on the Stokes number.

The reason for this phenomenon can be explained by analysing the fluid flow in a cross-section of the elbow. The fluid flow field in this region is shown in Fig. 7. We observe a structure of secondary flows (Dean vortices) that are responsible for centrifuging particles towards the wall, which may enhance erosion there. Similar observations were also made by other researchers. An example is a paper by Zeng et al. [14]. What differs their work from ours is that they did not consider the influence of particle size.

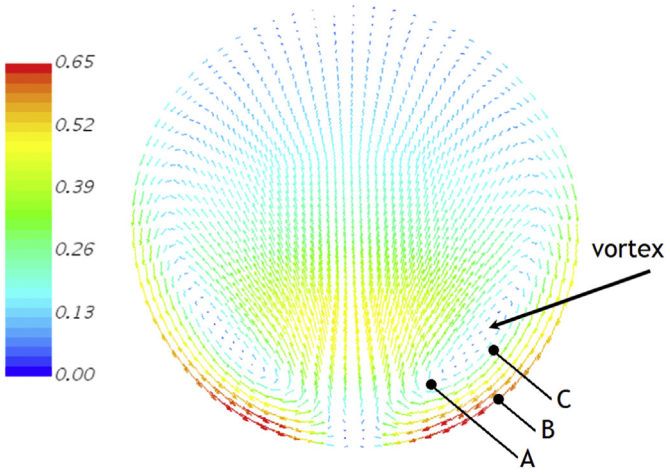

Fig. 7. Vortices created in the fluid in a cross-section of the elbow. Points A, B, C are monitor points in which the fluid velocity was evaluated for further analysis.

This phenomenon can be explained by analysing the fluid flow in a cross-section of the elbow, as shown in Fig. 7. Here, we observed a structure of secondary flows (Dean vortices) that was responsible for centrifuging particles towards the wall, which might enhance the erosion there. Zeng et al. [14] made similar observations, but unlike our work they did not consider the influence of particle size.

Peng et al. [38] also noticed an increase in the total erosion rate when the particle diameter was decreased. Nevertheless, they did not study particles of nano-metre size and therefore they did not report the existence of the local maximum as we observed in our research.

Gao et al. [20] investigated the impact of particle diameter and also found an increase in the erosion rate for smaller diameters. Their work, however, focused on rather different geometries, namely flows through heat exchangers. Therefore, it is interesting to note that the creation of secondary flows in various applications can influence the final outcome of the process.

This phenomenon occurred to a lesser degree for large particles that moved with the main flow and would not be captured by these secondary vortices. In Fig. 7 we show three points in the vortex area (A, B and C), in which we evaluated the magnitude of the fluid velocities. The results were around 0.7 m/s, 0.3 m/s, and 0.2 m/s. Also, the distance from these points to the centre of the vortex was estimated to be around 7 mm. These numbers made it possible to estimate some characteristic flow times. The results were 0.010 s, 0.023 s and 0.035 s. Similarly, we could calculate some characteristic time of the whole fluid flow by dividing the average velocity at the pipe inlet (1.0 m/s) by the pipe diameter giving a value of 0.0508 m/s.

The momentum response time of the particles used in the system was computed to be $1.65{\cdot}10^{-5}$s for particles with a diameter of 10^{-5}m, which was much less than any of the vortex characteristic times listed in the previous paragraph. This means that particles of this size will easily follow the flow in the vortices, that is, they will be centrifuged towards the wall of the pipe. In fact, the same thing will occur for even smaller particles but due to their small size they will not be able to erode the wall significantly. Thus, we obtained some critical value of particle diameter, which here was 10^{-5}m.

It is also interesting to note that larger particles, e.g. $3.0{\cdot}10^{-4}$m in diameter, had a momentum response time equal to 0.015 s. This was comparable with the vortex characteristic time, which indicated that these particles (and especially larger ones) were less subject to motion in the lateral direction that moves the particles towards the pipe wall.

When increasing the fluid velocity, the characteristic flow will decrease, while the momentum response time of the particles will remain constant. As a result, only smaller particles will follow the flow in the vortices. Therefore, the effect of the secondary flows on erosion may be rather observed for lower velocities in practice.

As mentioned previously, Shamshirband et al. [28] also studied flows laden with nano- and micro-particles through elbows. They focused on higher velocities in the system that resulted in higher Stokes numbers. Indeed, they observed the greatest erosion along the elbows extrados, and this might be why they did not report the local increase in the total erosion rate for particles with smaller diameters. For the larger particles, however, the tendency was similar to what we observed in our research, and similar conclusions were drawn in [29].

The existence of the secondary flows in elbows was also mentioned by Liu et al. [2]. They reported that the secondary flows shift the erosion wear to other locations in the pipe and this will influence the total erosion rate in the pipe, as observed by us.

4.4. Influence of coefficient of restitution

The influence of the coefficient of restitution on the erosion rate has not been widely studied. Most researchers use empirical relations that

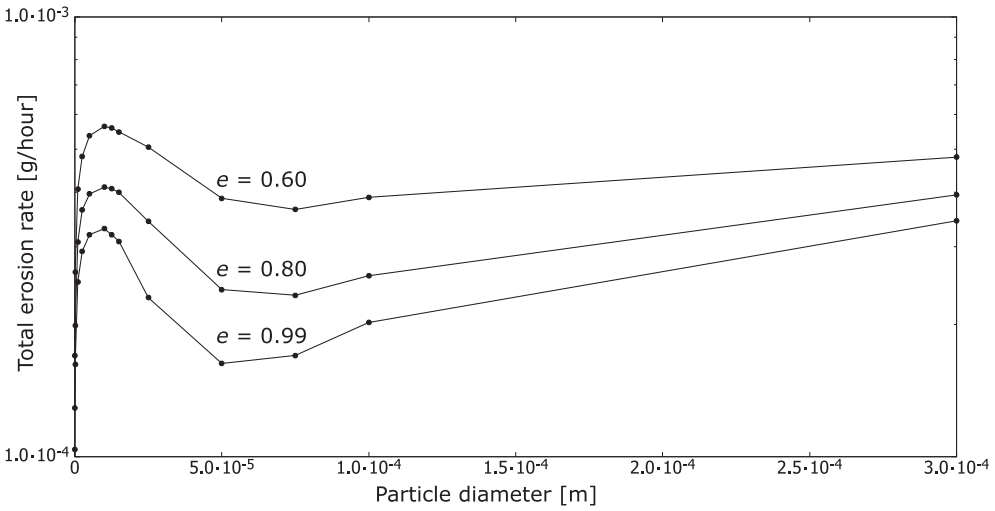

Fig. 8. The total erosion rate measured in the elbow after 1.4 s of the process (a steady flow was obtained) for various diameters and for different values of the coefficient of restitution.

are valid for the studied particle material, and the main advantage of this is that the results can be compared to experimental results.

In our research, however, we decided to use constant values of the coefficient so that we could investigate the influence of the different variables involved in collision events on the final erosion process in the pipe. For this, we tried three different values of the coefficient of restitution - 0.99, 0.80 and 0.60 - where the results for the first case are shown in the previous sections. As mentioned above, we used the same values of the coefficient along both the normal and tangential directions in order to simplify the model. Thus the final results are not obscured by multiple phenomena all occurring simultaneously.

It must be noted that the coefficients of restitution along the normal and tangential are not equal and not even constant in industrial applications. Not only depend they on particle material, but also on the impact velocity. In this paper, however, we decided to keep them constant and equal. As a results, we could mimick the loss of kinetic energy due to impact in a simple way and investigate its influence on the erosion process.

The results of the total erosion rate are shown in Fig. 8. The first observation is that a lower coefficient of restitution promoted the erosion. This confirms the statement discussed in the theoretical analysis in Section 2 that the probability that a subsequent encounter with the wall will occur increases because the particles are still close to the wall. In fact, this statement is further supported when comparing the total erosion rates for the largest particles. Here, the values of the total erosion rate differed less than for the smallest particles. For instance, for the case when the particle diameter was around $5{\cdot}10^{-5}$m, the ratio of the total erosion rate for the restitution coefficient 0.99 and 0.8 was around 0.8. For the case when the particle diameter increased to $3 \cdot 10^{-4}$m (the last point in the graph), the ratio increased to 0.87. Also, when the diameter was $1 \cdot 10^{-3}$m (not shown in the graph), the ratio became almost 1.0, i.e. we no longer observed any significant influence of the coefficient of restitution. This shows that large particles had enough inertia to leave the zone close to a solid surface after impact.

5. Concluding remarks

The focus of this paper was on assessing erosion rates for flows laden with nanoparticles. According to our results, the erosion rate for the smallest particles (e.g. of diameters less than 10^{-6}m) decreases with particle size, and this might indicate that the erosion risk is not significant. Nevertheless, this might not be the case in real-life applications. As mentioned previously, nano-size particles can easily form agglomerates whose size enters the micrometre range. Therefore, it is possible to reach the local maximum of the erosion rate.

Even though our model does not allow for the formation of agglomerates, it can still be stated that our simulations cover also flows of already formed agglomerates. These agglomerates are mimicked by the larger particles (i.e. of micro-size) that we also studied.

In addition, we note that for particle diameters around the "critical" diameter, the erosion occurs in certain concentrated areas. It must be noted that the concentration of erosion might also occur for other geometries, for instance, valves, pumps, etc. This means that flows with small particles might result in local damage to systems even though the small size of the particles might suggest that the flow as a whole is safe.

For validation of the software, we used experimental results from literature that do not cover all our computer simulations. The reason is that the issue of erosion due to very small particles is still unexplored. Nevertheless, the mathematical model as a whole consists of a series of well-established models. Also, some of our conclusions correspond well to what has been observed by other researchers. Therefore, we can state that our computer simulations are qualitatively correct. It must be noted, however, that there is a need to perform experiments that match our simulations.

Declaration of Competing Interest

The authors declare that they have no known competing financial interests or personal relationships that could have appeared to influence the work reported in this paper.

Acknowledgments

This study was supported by the Russian Science Foundation (project: 19-79-10083).

References

[1] M. Parsi, K. Najmi, F. Najafifard, S. Hassani, B.S. McLaury, S.A. Shirazi, A comprehensive review of solid particle erosion modeling for oil and gas wells and pipelines applications, J. Nat. Gas Sci. and Eng. 21 (2014) 850–873.
[2] J. Liu, W. Bakedashi, Z. Li, Y. Xu, W. Ji, C. Zhang, G. Cui, R. Zhang, Effect of flow velocity on erosion-corrosion of 90-degree horizontal elbow, Wear 376–377 (2017) 516–525.
[3] J. Neilson, A. Gilchrist, Erosion by a stream of solid particles, Wear 27 (2015) 706–718.
[4] G. Grant, W. Tabakoff, An experimental investigation of the erosion characteristics of 2024 aluminum alloy (tech. rep. 73-37), Tech. rep., Department of Aerospace Engineering, University of Cincinnati, 1973.

[5] Y. Oka, K. Okamura, T. Yoshida, Practical estimation of erosion damage caused by solid particle impact Part 1: effects of impact parameters on a predictive equation, Wear 259 (2005) 95–101.
[6] Det Norske Veritas, Recommended Practice RP, vol. 0501, Erosive wear in piping systems, Tech. rep, 2007.
[7] Y. Zhang, E.P. Reuterfors, B.S. McLaury, S.A. Shirazi, E.F. Rybicki, Comparison of computed and measured particle velocities and erosion in water and air flows, Wear 263 (2007) 330–338.
[8] A. Mansouri, Development of erosion equations for slurry flows. advisory board report, Tech. rep., Erosion/Corrosion Research Center, The University of Tulsa, 2015.
[9] M. Parsi, M. Agrawal, V. Srinivasan, R. Vieira, C. Torres, B. McLaury, S. Shirazi, CFD simulation of sand particle erosion in gas-dominant multiphase flow, J. Nat.Gas Sci. Eng. 27 (2015) 706–718.
[10] X. Song, P. Luo, S. Luo, S. Huang, Z. Wang, Numerical simulation study on the influence of incident position on erosion characteristics of gas-particle two-phase flow in 90 elbow, Adv. Mech. Eng. 9 (10) (2017) 1–18.
[11] M. Zamani, S. Seddighi, H. Nazif, Erosion of natural gas elbows due to rotating particles in turbulent gas-solid flow, J. Nat.Gas Sci. Eng. 40 (2017) 91–113.
[12] M. Banakermani, H. Naderan, M. Saffar-Avval, An investigation of erosion prediction for 15° to 90° elbows by numerical simulation of gas-solid flow, Powder Technol. 334 (2018) 9–26.
[13] J. Zhou, Y. Liu, S. Liu, C. Du, J. Li, Effects of particle shape and swirling intensity on elbow erosion in dilute-phase pneumatic conveying, Wear 380–381 (2017) 66–77.
[14] D. Zeng, E. Zhang, Y. Ding, Y. Yi, Q. Xian, G. Yao, H. Zhu, T. Shi, Investigation of erosion behaviors of sulfur-particle-laden gas flow in an elbow via a cfd-dem coupling method, Powder Technol. 329 (2018) 115–128.
[15] J. Zhang, B.C. McLaury, S.A. Shirazi, Application and experimental validation of a CFD based erosion prediction procedure for jet impingement geometry, Wear 394–395 (2018) 11–19.
[16] R. Aponte, L. Teran, J. Ladino, F. Larrahondo, J. Coronado, S. Rodriguez, Computational study of the particle size effect on a jet erosion wear device, Wear 374-375 (2016) 97–103.
[17] N. Lin, H. Arabnejad, S. Shirazi, B. McLaury, H. Lan, Experimental study of particle size, shape and particle flow rate on erosion of stainless steel, Powder Technol. 336 (2018) 70–79.
[18] H. Arabnejad, S.A. Shirazi, B.S. McLaury, H.J. Subramani, L.D. Rhyne, The effect of erodent particle hardness on the erosion of stainless steel, Wear 332–333 (2015) 1098–1103.
[19] V.B. Nguyen, Q.B. Nguyen, Y.W. Zhang, C.Y.H. Lim, B.C. Khoo, Effect of particle size on erosion characteristics, Wear 349–349 (2016) 126–137.
[20] W. Gao, Y. Li, L. Kong, Numerical investigation of erosion of tube sheet and tubes of a shell and tube heat exchanger, Comput. Chem. Eng. 96 (2017) 115–127.
[21] T.A. Sedrez, R.K. Decker, M.K. da Silva, D. Noriler, H.F. Meier, Experiments and CFD-based erosion modeling for gas-solids flow in cyclones, Powder Technol. 311 (2017) 120–131.
[22] M. Azimian, H.J. Bart, Numerical analysis of hydroabrasion in a hydrocyclone, Pet. Sci. 13 (2016) 304–319.
[23] Y. Perelstein, E. Gutmark, A numerical investigation of wear caused by dilute slurry injected into an annulus through rectangular apertures, Wear 364–365 (2016) 169–183.
[24] A. Kosinska, Interaction of debris with a solid obstacle: numerical analysis, J. Hazard. Mater. 177 (2010) 602–612.
[25] S.U.S. Choi, J.A. Eastman, Anomalous thermal conductivity enhancement in nanotube suspensions, Tech. rep., Department of Aerospace Engineering, University of Cincinnati, 2001.
[26] E.T. Ulset, P. Kosinski, Y. Zabednova, O.V. Zhdaneev, P.G. Struchalin, B.V. Balakin, Photothermal boiling in aqueous nanofluids, Nano Energy 50 (2018) 339–346.
[27] B.V. Balakin, O.V. Zhdaneev, A. Kosinska, K.V. Kutsenko, Direct absorption solar collector with magnetic nanofluid: CFD model and parametric analysis, Renew. Energy 136 (2019) 23–32.
[28] S. Shamshirband, A. Malvandi, A. Karimipour, M. Goodarzi, M. Afrand, D. Petkovic, M. Dahari, N. Mahmoodian, Performance investigation of micro- and nano-sized particle erosion in a 90 elbow using an anfis model, Powder Technol. 284 (2015) 336–343.
[29] M.R. Safaei, O. Mahian, F. Garoosi, K. Hooman, A. Karimipour, S.N. Kazi, S. Gharehkhani, Investigation of micro- and nanosized particle erosion in a 90° pipe bend using a two-phase discrete phase model, Sci. World J. 2014 (2014) https://doi.org/10.1155/2014/740578 (Art. ID 740578, 12 pages).
[30] M.M. Asifa, Numerical assessment of the effect nanofluids on the erosion and corrosion in the radiator pipes by using coolant fluids, Iraqi J. Mech. and Mat. Eng. 16 (2016) 377–393.
[31] G.J. Molina, F. Aktaruzzaman, W. Stregles, V. Soloiu, M. Rahman, Jet-impingement effects of alumina-nanofluid on aluminum and copper, Adv. Tribol. 2014 (2014) https://doi.org/10.1155/2014/476175 (Art. ID 476175, 8 pages).
[32] G. Desale, B. Gandhi, S. Jain, Particle size effects on the slurry erosion of aluminium alloy (aa 6063), Wear 266 (2009) 1066–1071.
[33] C. Crowe, M. Sommerfeld, Y. Tsuji, Multiphase Flow with Droplets and Particles, CRC Press, 1998.
[34] C. Duarte, F. de Souza, V. dos Santos, Mitigating elbow erosion with a vortex chamber, Powder Technol. 288 (2016) 6–25.
[35] C. Duarte, F. de Souza, R. Salvo, V. dos Santos, The role of inter-particle collisions on elbow erosion, Int. J. Multiphase Flow 89 (2017) 1–22.
[36] L. Xu, Q. Zhang, J. Zheng, Y. Zhao, Numerical prediction of erosion in elbow based on CFD-DEM simulation, Powder Technol. 302 (2016) 236–246.
[37] Y. Oka, T. Yoshida, Practical estimation of erosion damage caused by solid particle impact Part 2: mechanical properties of materials directly associated with erosion damage, Wear 259 (2005) 102–109.
[38] W. Peng, X. Cao, Numerical simulation of solid particle erosion in pipe bends for liquid-solid flow, Powder Technol. 294 (2016) 266–279.
[39] Q.H. Mazumder, S.A. Shirazi, B. McLaury, Experimental investigation of the location of maximum erosive wear damage in elbows, J. Press. Vessel. Technol. 130 (2008) (011303-1 – 011303-7).